Isoform-Selective Interaction of Cyclooxygenase-2 with Indomethacin Amides Studied by Real-Time Fluorescence, Inhibition Kinetics, and Site-Directed Mutagenesis†

Sergei L. Timofeevski, Jeffery J. Prusakiewicz, Carol A. Rouzer, and Lawrence J. Marnett*

Departments of Biochemistry and Chemistry, Center in Molecular Toxicology, Vanderbilt−Ingram Cancer Center, Vanderbilt University School of Medicine, Nashville, Tennessee 37232

Received May 15, 2002

ABSTRACT: Conversion of carboxylate-containing nonsteroidal antiinflammatory drugs, such as indomethacin, to esters or amides provides potent and selective inhibitors of cyclooxygenase-2 (COX-2) [Kalgutkar et al. (2000) *Proc. Natl. Acad. Sci. U.S.A. 97*, 925−930]. Synthesis of cinnamyl- or coumarinyl-substituted ethanolamide derivatives of indomethacin produced fluorescent probes of inhibitor interaction with COX-2 and COX-1. Binding of either derivative to apoCOX-2 or apoCOX-1 resulted in a rapid, reversible enhancement of fluorescence. Following this rapid phase, a slow additional increase in fluorescence was observed with apoCOX-2 but not with apoCOX-1. The slow, COX-2-specific increase in fluorescence was prevented or reversed by addition of the nonfluorescent COX inhibitor (*S*)-flurbiprofen. Detailed kinetic studies of the interaction of the coumarinyl derivative with COX-2 showed that the observed changes in fluorescence could be described by two sequential equilibria, the first of which is rapid, reversible, and bimolecular in the forward direction. The second equilibrium is slower, reversible, and unimolecular in both directions. The forward rate constant for the slow equilibrium determined by fluorescence enhancement [$(3.1 \pm 0.6) \times 10^{-3}$ s^{-1}] corresponded closely to the forward rate constant for inhibition of COX-2 activity [$(6.8 \pm 2.3) \times 10^{-3}$ s^{-1}], suggesting that the slow fluorescence enhancement is associated with selective COX-2 inhibition. Site-directed mutagenesis indicated that residues in the carboxylate-binding region of the COX-2 active site (Arg-120, Tyr-355, and Glu-524) are critical for the binding of the indomethacin conjugates that leads to slow fluorescence enhancement and cyclooxygenase inhibition. The indomethacin conjugates described herein represent powerful tools for the investigation of a novel class of selective inhibitors of COX-2.

Cyclooxygenase-2 (COX-2)[1] has emerged as an important molecular target for the development of antiinflammatory, analgesic, cancer chemopreventive, and antiangiogenic agents (*1*, *2*). Three selective COX-2 inhibitors (celecoxib, rofecoxib, and valdecoxib) are currently marketed, and they demonstrate superior safety profiles compared to conventional nonsteroidal antiinflammatory drugs (NSAIDs), which inhibit both COX-2 and COX-1 (*3*, *4*). The improved therapeutic ratio of COX-2 inhibitors appears to be due to their inability to inhibit COX-1 in the gastrointestinal tract. Celecoxib, rofecoxib, and valdecoxib are diaryl heterocycles that contain a sulfonamide or sulfone in one of the aromatic rings (*5*, *6*). Sulfonyl substitution confers isoform selectivity by insertion into a binding pocket on the side of the cyclooxygenase active site; this side pocket is only present in COX-2 (*7*, *8*).

Our group recently described a facile strategy for the development of COX-2 inhibitors based on the observation that neutral derivatives of some carboxylic acid-containing NSAIDs (e.g., indomethacin, meclofenamic acid) bind efficiently to COX-2 but not to COX-1 (*9*, *11*). The molecular basis for selectivity is not clear but appears to involve hydrogen bonding to residues in the carboxylate-binding region of the cyclooxygenase active site (*9*). Indomethacin esters and amides do not bind in the side pocket as diaryl heterocycles do but may breach the constriction at the base of the cyclooxygenase active site comprised of Arg-120, Tyr-355, and Glu-524 (*8*). The tethered ester or amide functional group projects down into a spacious cavity in the membrane binding domain that we term the lobby. This structural model is consistent with the breadth of substituted ester and amide groups that can be tethered to indomethacin while maintaining COX-2 selectivity (*10*).

Fluorescent techniques have been employed for studying the dynamics of the interaction of COX-2 with inhibitors (*12*−*14*). Our laboratory previously utilized fluorescence quenching to probe the binding and release of a COX-2 selective diaryl heterocycle (SC299) (*14*). That study revealed that SC299 binds to both COX-1 and COX-2 with comparable rates. Binding to COX-1 can be modeled by sequential bimolecular and unimolecular reactions that are both rapidly reversible. Binding to COX-2 is qualitatively similar but

† This work was supported by Research and Program Grants from the National Institutes of Health (CA89450 and CA86283).

* To whom correspondence should be addressed. Telephone: 615-343-7329. Fax: 615-343-7534. E-mail: marnett@toxicology.mc.vanderbilt.edu.

[1] Abbreviations: COX, cyclooxygenase [prostaglandin endoperoxide synthase, prostaglandin G/H synthase (EC 1.14.99.1)]; wt COX, wild-type cyclooxygenase; LM-4134, *N*-[4-(*N*,*N*-dimethylamino)cinnamyloxyethyl]-1-*p*-chlorobenzoyl-5-methoxy-2-methylindole-3-acetamide; LM-4143, *N*-[7-(*N*,*N*-diethylamino)coumarin-3-carbonyloxyethyl]-1-*p*-chlorobenzoyl-5-methoxy-2-methylindole-3-acetamide; NSAIDs, nonsteroidal antiinflammatory drugs.

10.1021/bi0203637 CCC: $22.00
Published on Web 07/04/2002

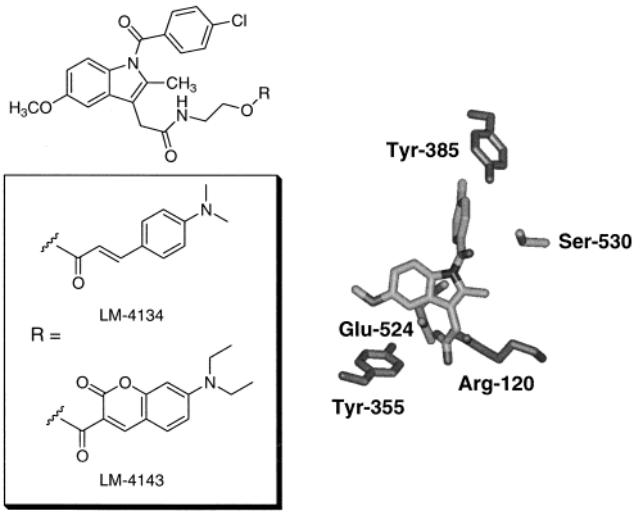

FIGURE 1: Structures of LM-4143 and LM-4134 and the structure of indomethacin in complex with key residues of COX-2 (from ref *7*).

exhibits a second unimolecular step that appears to reflect binding in the side pocket. The second unimolecular step is very slowly reversible, which accounts for the COX-2 selectivity of the inhibitor (*14*).

To study the kinetics and selectivity of binding of neutral derivatives of NSAIDs to COX-2, we synthesized indomethacin derivatives containing fluorophores attached to the carboxyl group through an amide linkage. Several candidate amides were screened to find a cinnamyl and a coumarinyl derivative that were promising for further kinetic analysis (Figure 1). These amides are very weakly fluorescent in aqueous solution, but on binding to apoCOX-1 or apoCOX-2 they exhibit rapid increases in fluorescence. This is followed by a further enhancement of fluorescence of the inhibitor complex that is selective for apoCOX-2. The second phase of fluorescence enhancement parallels the development of COX-2 inhibition. We have studied the kinetics of binding and release of the coumarinyl inhibitor to apoCOX-2, apoCOX-1, and a series of site-directed mutants of apoCOX-2 that affect sensitivity to enzyme inhibition. The results provide a detailed picture of the dynamics of the interaction of this novel class of molecules that leads to COX-2 inhibition.

MATERIALS AND METHODS

Chemistry

Materials. Indomethacin and hematin were purchased from Sigma Chemical Co. (St. Louis, MO). 7-Diethylaminocoumarin-3-carboxylic acid was obtained from Molecular Probes, Inc. (Eugene, OR). (*S*)-Flurbiprofen was from Pharmacia (Kalamazoo, MI). Arachidonic acid was purchased from Nu Chek Prep (Elysian, MN). [1-^{14}C]Arachidonic acid was purchased from American Radiolabeled Chemicals (ARC, St. Louis, MO). All other chemicals and solvents were obtained from Aldrich (Milwaukee, WI). Analytical thin-layer chromatography on Uniplate silica gel plates (Analtech, Newark, DE) was used to monitor the course of synthetic reactions. Silica gel (Fisher, 60−100 mesh) was used for column chromatography.

Spectroscopy. ^{1}H NMR spectra in $CDCl_3$ or DMSO-d_6 were recorded on a Bruker WP-360 or AM-400 spectrometer; chemical shifts are expressed in parts per million (ppm, δ) relative to tetramethylsilane as internal standard. Spin multiplicities are given as s (singlet), br s (broad singlet), d (doublet), dd (doublet of doublets), t (triplet), and q (quartet). Positive ion electrospray (ESI) and collision-induced dissociation (CID) mass spectra were recorded on a Finnigan TSQ 7000 instrument. CID fragmentations were consistent with assigned structures.

N-[4-(N,N-Dimethylamino)cinnamyloxyethyl]-1-p-chlorobenzoyl-5-methoxy-2-methylindole-3-acetamide (LM-4134) and N-(2-hydroxyethyl)-1-p-chlorobenzoyl-5-methoxy-2-methylindole-3-acetamide were synthesized as reported previously (*10*). ϵ_{max} (LM-4134) = 2.0×10^4 M^{-1} cm^{-1} at 380 nm (0.1 M Tris, pH 8) and 3.0×10^4 M^{-1} cm^{-1} at 364 nm (CH_3CN).

N-[7-(N,N-Diethylamino)coumarin-3-carbonyloxyethyl]-1-p-chlorobenzoyl-5-methoxy-2-methylindole-3-acetamide (LM-4143). To a solution of 7-diethylaminocoumarin-3-carboxylic acid (66 mg, 0.25 mmol) in dry CH_2Cl_2 (2 mL) was added 1-[3-(dimethylamino)propyl]-3-ethylcarbodiimide hydrochloride (65 mg, 0.33 mmol) and 4-(dimethylamino)pyridine (3.3 mg, 0.027 mmol) followed by *N*-(2-hydroxyethyl)-1-*p*-chlorobenzoyl-5-methoxy-2-methylindole-3-acetamide (109 mg, 0.272 mmol). The reaction was stirred at room temperature overnight. The reaction mixture was diluted with CH_2Cl_2 (25 mL), then washed with water (3 × 25 mL), dried ($MgSO_4$), filtered, and concentrated in vacuo. The crude product was purified by chromatography on silica gel (EtOAc:hexanes, 2:1, to EtOAc) and obtained as a bright yellow solid (48 mg, 27%). ESI-CID calcd for $C_{35}H_{34}ClN_3O_7$ (MH^+) 644.2, (MNa^+) 666.2; found (MH^+) 644.3, (MNa^+) 666.2; *m/z* 633.9, 630.1, 607.2, 383.3, 312.1, 244.2, 139.0. ^{1}H NMR ($CDCl_3$) δ 8.23 (s, 1 H, ArH), 7.83−7.86 (d, 2 H, J = 8.5 Hz, ArH), 7.50−7.53 (d, 2 H, J = 8.4 Hz, ArH), 7.38−7.41 (d, 1 H, J = 8.8 Hz, ArH), 6.80−6.81 (d, 1 H, J = 2.5 Hz, ArH), 6.71−6.74 (d, 1 H, J = 9.0 Hz, ArH), 6.66 (br s, 1 H, NH), 6.59 (br s, 1 H, ArH), 6.44 (s, 1 H, ArH), 6.30−6.34 (dd, 1 H, J = 8.9 and 2.3 Hz, ArH), 4.30−4.33 (t, 2 H, J = 4.8 Hz, CH_2), 3.76 (s, 3 H, CH_3), 3.65 (br s, 4 H, $2CH_2$), 3.43−3.50 (q, 4 H, J = 7.0 Hz, $2CH_2$), 2.38 (s, 3 H, CH_3), 1.23−1.28 (t, 6 H, J = 7.0 Hz, $2CH_3$). ϵ_{max} = 2.6×10^4 M^{-1} cm^{-1} at 435 nm (0.1 M Tris, pH 8) and 4.1×10^4 M^{-1} cm^{-1} at 417 nm (CH_3CN).

Enzymology

Proteins. COX-1 was purified from ram seminal vesicles (Oxford Biomedical Research, Inc., Oxford, MI) as described previously (*15*). Murine wild-type COX-2 and mutant COX-2 enzymes were expressed in *Sf*-9 insect cells using a pVL1393 expression vector (Pharmingen, San Diego, CA) and purified by ion-exchange and size-exclusion chromatography as previously reported (*16*). All purified proteins were at least 80% pure by densitometry of polyacrylamide gels. Enzyme concentrations are specified per monomer. Holoenzymes were prepared by the addition of hematin to purified apoenzymes.

Time- and Concentration-Dependent and Competitive Inhibition of COX. The cyclooxygenase activity of ovine COX-1 or murine COX-2 was assayed by thin-layer chromatography as previously described (*10*). Inhibition assays were performed at 25 °C, except for IC_{50} determinations, which were performed at 37 °C. In time-dependent inhibition

assays, 0.15 μM enzyme was preincubated with 0−25 μM inhibitor for 0.1−32 min followed by incubation with 50 μM [1-^{14}C]arachidonate for 15 s, unless otherwise specified. Kinetic parameters were calculated as described in the text. Competitive inhibition was performed with 0.5−5 μM substrate, added to the enzyme simultaneously with the inhibitor. In all inhibition assays, the enzyme concentration was adjusted to allow no more than 50% conversion of substrate to products. Enzymes were reconstituted with heme (1−5 μM final concentration) prior to incubation with inhibitor. Alternatively, hematin (10 μM final concentration) was combined with substrate and added to enzyme samples following incubation of apoenzyme with inhibitor, as described elsewhere (*12*).

Steady-State Fluorescence Spectroscopy. Steady-state fluorescence excitation and emission spectra of indomethacin derivatives were obtained with a Spex 1681 Fluorolog spectrofluorometer, equipped with a 450 W xenon arc lamp. The excitation and emission monochromator slit widths were 1−2 mm. Background fluorescence from solvent alone, apoprotein, and holoprotein was recorded and subtracted from the fluorophore samples. Steady-state measurements were performed at 25 °C in a 0.15 mL fluorescence cuvette with 2 mm excitation and 10 mm emission path lengths. The fluorophores were dissolved in CH_3CN before further dilution into buffer. The amount of organic solvent in buffers in the presence of protein was kept below 6%. Quantum yields were determined by a published procedure using quinine sulfate as a reference compound ($\Phi = 0.55$ in 1 N H_2SO_4) (*17*). Steady-state anisotropy measurements were performed with the same instrument. Excitation was at 375 nm for LM-4134 and 420 nm for LM-4143, and polarized fluorescence was measured at 450 nm for LM-4134 and 470 nm for LM-4143. Anisotropy was calculated as previously described (*18*).

Kinetics of Binding of Indomethacin Amides to COX Isoforms. Reactions were performed at 25 °C in a Spex 1681 Fluorolog spectrofluorometer or Applied Photophysics SX.18MV stopped-flow unit with a 100 μL cuvette and autostop assembly. Excitation was at 420 nm (400 nm on the stopped-flow instrument) for LM-4143, and 375 nm for LM-4134, and was polarized at 35.3° to eliminate polarization bias (*19*). Fluorescence emission was detected at 463 and 445 nm for LM-4143 and LM-4134, respectively, in the fluorometer or through a 420 nm cutoff filter in the stopped-flow instrument using a Hamamatsu emission photomultiplier with high voltage. Slit widths were set to 0.8−2 mm on the fluorometer for excitation and emission and 2−4 mm for excitation on the stopped-flow instrument. Background fluorescence from solvent alone, inhibitor, apoprotein, or holoprotein was recorded and subtracted from the fluorophore samples, as appropriate. Kinetic traces were acquired at least in triplicate. Observed rate constants for the interaction of the inhibitor with apoenzyme were determined from single-exponential fits to respective kinetic traces obtained under conditions in which the change in free inhibitor concentration was less than 10%. The analyses were performed using Prism GraphPad. In fluorescence titration experiments, the fluorescence increase was recorded upon mixing of the inhibitor with apoenzyme, using either an excess of inhibitor or an excess of enzyme while the other reactant was kept constant at 0.03−0.05 μM.

Kinetics of Dissociation of Indomethacin Amides from ApoCOX-2. The dissociation of fluorescent inhibitors from apoCOX-2 was monitored by the decrease in fluorescence intensity of the inhibitor following the addition of various amounts of (*S*)-flurbiprofen. The measurements were carried out in a Spex 1681 Fluorolog instrument as described above for binding kinetics. The data were background corrected and computer fitted to a single-exponential equation.

RESULTS

Kinetics of Inhibition of COX-2 by Fluorescent Indoamides. The fluorescent indomethacin amides, LM-4134 and LM-4143 (Figure 1), were prepared as described under Materials and Methods. Consistent with our results on a wide variety of other indomethacin amides and esters (*10*), both compounds were selective, time-dependent COX-2 inhibitors. The IC_{50} values for COX-2 were 0.25 μM with LM-4134 and 2.2 μM with LM-4143, whereas no significant inhibition was observed for either inhibitor with COX-1 ($IC_{50} > 100$ μM). Due to the higher quantum yield of fluorescence of LM-4143 (see below), this compound was selected for detailed kinetic study.

The time-dependent inhibition of wild-type holoCOX-2 by LM-4143 obeyed first-order kinetics (Figure 2A). Similar data were obtained in experiments when apoCOX-2 was preincubated with inhibitor followed by the addition of excess heme simultaneously with substrate (data not shown). This result indicated that the binding kinetics of the inhibitor with apoenzyme were identical to those with heme-reconstituted enzyme and that the interaction of the compound with either enzyme form resulted in inhibition. Values for the observed first-order rate constants (k_{obs}) for enzyme inhibition were obtained over a range of LM-4143 concentrations. A plot of these data (Figure 2B) yielded a hyperbolic function with a nonzero *y*-intercept. These findings suggest that the inhibition of the enzyme by LM-4143 results from an interaction of the compound with the enzyme that can be described by a two-step mechanism in which a rapidly reversible bimolecular association is followed by a slowly reversible unimolecular transition to yield the inhibited enzyme complex, E−I* (*20*):

$$E + I \underset{k_{-1}}{\overset{k_1}{\rightleftharpoons}} E{-}I \underset{k_{-2}}{\overset{k_2}{\rightleftharpoons}} E{-}I^* \qquad (1)$$

where $k_{-1} \gg k_2$. According to this model the data may be described by eq 2. Thus, in Figure 2, the *y*-intercept is equal to k_{-2}, the amplitude of the hyperbolic increase is equal to k_2, and the value at one-half the maximum of the hyperbolic increase of k_{obs} is equal to the dissociation constant, $K_D = k_{-1}/k_1$, for the initial complex, respectively. These values, obtained by nonlinear regression analysis using eq 2, are summarized in Table 1. Note that the error in the estimated

$$k_{obs} = \frac{k_2[I]}{K_D + [I]} + k_{-2} \qquad (2)$$

kinetic parameters shown in Table 1 is quite high. This is due to the difficulty in obtaining accurate values for k_{obs} in the activity inhibition assay. As seen in Figure 2, at low concentrations of inhibitor, the level of inhibition achieved upon reaching equilibrium is in the range of only 15−20%.

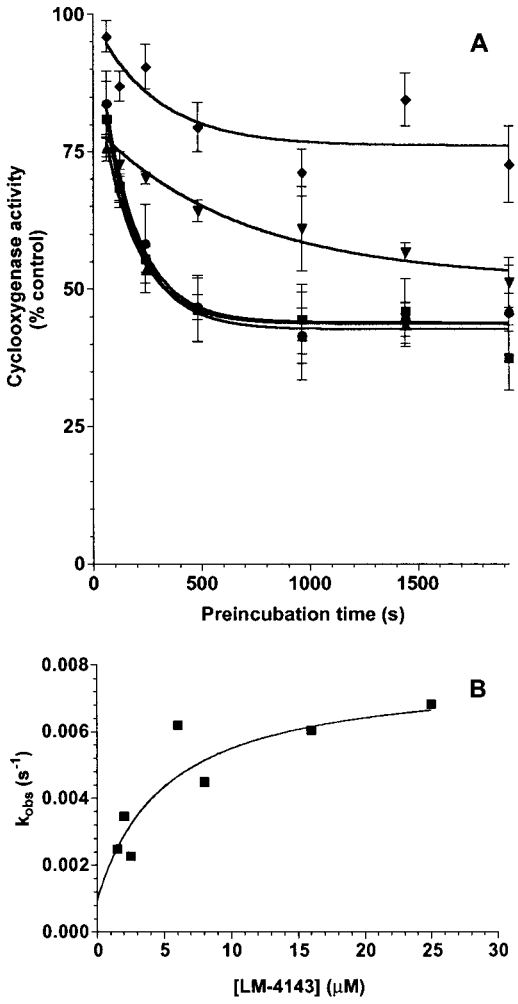

FIGURE 2: Kinetics of the time-dependent inhibition of COX-2 by LM-4143. (A) Murine COX-2 (0.15 μM), reconstituted with heme, was preincubated with the indicated amounts of LM-4143 for various periods of time, and the cyclooxygenase activity was calculated relative to that of uninhibited enzyme. The activity values were fitted to an exponential equation to obtain values for k_{obs} for 2 μM (◆), 4 μM (▼), 6 μM (●), 8 μM (■), and 16 μM (▲) LM-4143. (B) The observed first-order rate constants were plotted versus inhibitor concentration, and the data were analyzed by nonlinear regression to fit a hyperbolic equation with a floating *y*-intercept, as described in the text. Further experimental details are given under Materials and Methods.

Table 1: Kinetic Constants for the Interaction of LM-4143 with COX-2[a]

by fluorescence			by inhibition		
$k_2 \times 10^3$ (s^{-1})	$k_{-2} \times 10^3$ (s^{-1})	K_D (μM)	$k_2 \times 10^3$ (s^{-1})	$k_{-2} \times 10^3$ (s^{-1})	K_D (μM)
3.1± 0.6[b]	1.9 ± 0.3[b]	3.1 ± 2.3[b]	6.8 ± 2.3	1.0 ± 3.3	5 ± 10
	2.3 ± 0.1[c]	1.1 ± 0.4[d]			

[a] Kinetic parameters were determined as described in the text and legends to Figures 2 and 6−8 and reported with standard errors of the fits. [b] From kinetic analysis of the slow phase fluorescence change. [c] From competition with (*S*)-flurbiprofen. [d] From the rapid reaction by fluorescence titration.

Thus, the inhibition values at early time points are close to the error in the assay (approximately 5%). Obtaining values of k_{obs} at high concentrations of inhibitor is limited by compound solubility. Since the nonlinear regression analysis used to obtain k_2, k_{-2}, and K_D involves the determination of three parameters, relatively small errors in the data points may lead to a large error in the resulting values.

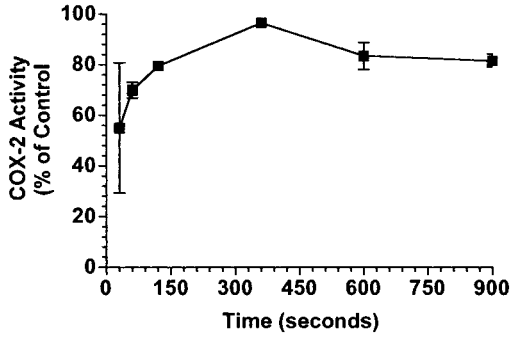

FIGURE 3: Reversibility of inhibition of COX-2 by LM-4143. Murine holoCOX-2 (0.05 μM) was preincubated with or without 10 μM LM-4143 for 20 min, and the cyclooxygenase activity was assayed by incubating the enzyme with 50 μM 1-^{14}C-labeled arachidonic acid for various times. The activity was expressed relative to uninhibited enzyme. The data points represent two independent measurements, and error bars represent the range. The experiments were carried out as described under Materials and Methods.

The nonzero *y*-intercept in Figure 2 indicates that the second equilibrium is reversible. This is in contrast to many other time-dependent COX inhibitors which form an essentially irreversible complex with the enzyme (*13*, *14*, *21*−*23*). The reversibility of the interaction of LM-4143 with COX-2 is confirmed by the nonzero residual cyclooxygenase activity upon preincubation of COX-2 with excess inhibitor (Figure 2) and the reversibility of inhibition observed upon increasing the time of incubation with saturating concentrations of arachidonic acid (Figure 3). The cyclooxygenase activity (with respect to uninhibited enzyme) was recovered as the time of the incubation with arachidonic acid increased (at an [arachidonate]/[LM-4143] = 10). Similar experiments using 10 μM indomethacin as the inhibitor showed no such recovery of activity (data not shown).

The relatively high cyclooxygenase activities observed in experiments with no inhibitor preincubation (Figure 2) indicated that LM-4143 is a poor competitive inhibitor. Indeed, when enzyme was added last to a reaction mixture containing both inhibitor and substrate, no significant inhibition of COX-2 was detected with up to 80 μM inhibitor (data not shown). Therefore, the initial bimolecular interaction of COX-2 with LM-4143 suggested by the kinetic data (eq 1) likely does not result in inhibition. Rather, inhibition must depend on the second step of the interaction. Similar behavior has been seen with other indomethacin derivatives that are selective COX-2 inhibitors (*9*).

Fluorescence Properties of LM-4143 and LM-4134 and Their Complexes with COX-1 and COX-2. The finding that LM-4143 and LM-4134 are selective COX-2 inhibitors indicated that they must specifically interact with the enzyme. Thus, it was of interest to determine whether this interaction could be observed as a change in the fluorescence properties of the compounds. Characterization of the fluorescence behavior of the inhibitors showed that the excitation and emission wavelength maxima and quantum yields were strongly dependent on solvent, with marked blue shifts and fluorescence enhancement in CH_3CN, compared to Tris buffer (Table 2). The steady-state fluorescence anisotropies of the amides were higher in aqueous solution than in organic

Table 2: Effect of Environment on the Fluorescence Properties of Coumarinyl and Cinnamyl Derivatives of Indomethacin[a]

	LM-4143				LM-4134			
environment	Φ	λ_{ex}	λ_{em}	*r*	Φ	λ_{ex}	λ_{em}	*r*
acetonitrile	0.11	419	465	0.13	0.047	368	460	0.17
0.1 M Tris, pH 8	0.03	439	478	0.31	0.003	380	483	0.24
apoCOX-2	0.52	429	463	0.36	0.058[b]	376	444	0.38
apoCOX-1	0.17[b]	427	465	0.34	0.02[b]	379	456	0.37

[a] The quantum yield (Φ), excitation and emission wavelength maxima (λ_{ex} and λ_{em}, nm), and steady-state anisotropy (*r*) were determined as described under Materials and Methods. [b] Calculated by fluorescence titration for the inhibitor bound to the enzyme following the slow reaction with apoCOX-2 or rapid reaction with apoCOX-1.

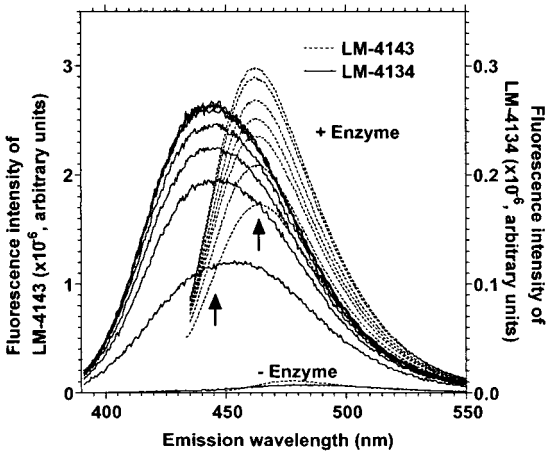

FIGURE 4: Fluorescence emission spectra of indomethacin amides during incubation with apoCOX-2. The emission spectra of 0.5 μM LM-4134 (solid lines) or LM-4143 (dashed lines) were recorded at 1, 3, 5, 9, 13, 20, and 30 min, as shown by arrows, following mixing with 2 μM apoCOX-2 in 0.1 M Tris buffer, pH 8. The fluorescence of LM-4134 or LM-4143 was excited at 375 or 420 nm, respectively. The emission spectra were background corrected.

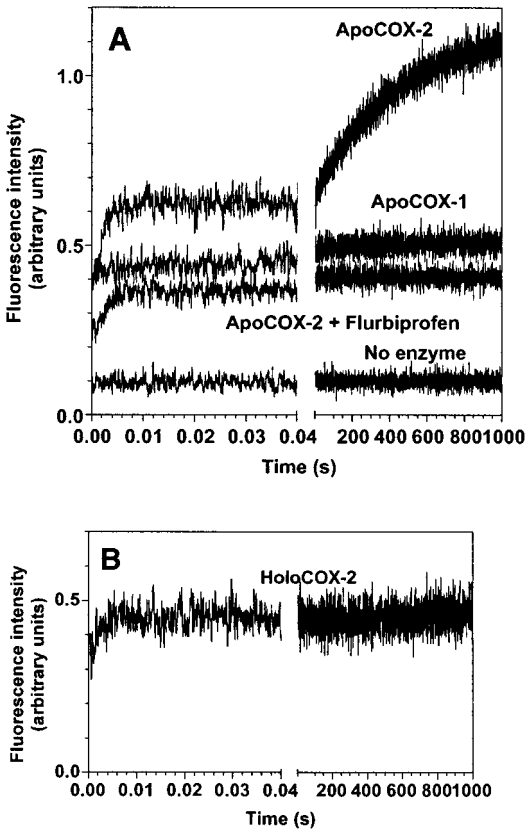

FIGURE 5: Time courses of association of LM-4143 with COX-1 and COX-2 apoenzymes, monitored by fluorescence of the inhibitor. (A) Binding to apoCOX-2 and apoCOX-1. Stopped-flow kinetic traces of the fluorescence intensity of LM-4143 were recorded with 2 μM LM-4143 and one of the following: 2 μM apoCOX-2; 2 μM apoCOX-2 preincubated with 1 mM (*S*)-flurbiprofen; 2 μM apoCOX-1; or no enzyme. (B) Binding to holoCOX-2. The fluorescence was recorded following the mixing of 2 μM LM-4143 with 2 μM holoCOX-2. Data were corrected for buffer and protein backgrounds, as appropriate. The experiments were performed as described under Materials and Methods.

solvent, exceeding 0.3 for LM-4143 in buffer (Table 2). In contrast, the parent 7-(diethylamino)coumarin-3-carboxylic acid had anisotropy values of 0.10 and 0.15 in CH_3CN and Tris, respectively, suggesting that the indomethacin moiety decreased the rotational diffusion of the fluorescent groups by increasing molecular aggregation in buffer.

During incubation with apoCOX-2, both indomethacin derivatives exhibited a large increase in fluorescence, which developed during an initial rapid phase followed by a slower phase (Figures 4 and 5A). The rapid phase observed with apoCOX-2 was also observed with holoCOX-2. However, a slower increase in fluorescence was not detected with holoCOX-2, because of the quenching of the fluorescence by the heme prosthetic group (Figure 5B). On incubation with apoCOX-1, a rapid increase in fluorescence was observed but a slower increase was not (Figure 5A). The rapid increase in fluorescence observed with apoCOX-2 and apoCOX-1 was not due to residual detergent in the enzyme preparations. Addition of an identical volume of detergent-containing buffer (0.1% CHAPS or 0.1% Tween-20) in the absence of protein led to an increase of only 10% that observed in the presence of 0.5 M apoCOX-2 or apoCOX-1.

The quantum yields of LM-4134 and LM-4143 were nearly 20-fold higher when they were bound to apoCOX-2 than when they were dissolved in buffer (Table 2). The end-point emission maxima were blue shifted by 15−39 nm with apoCOX-2 and 13−27 nm with apoCOX-1 (Table 2, Figure 4). The steady-state fluorescence anisotropies of the compounds increased upon incubation with apoenzymes relative to compounds in buffer (Table 2). There was only a small difference in the end-point anisotropy value of compounds bound to COX-2 compared to COX-1 (Table 2), and the anisotropies increased only by ∼0.005 following the rapid association with either enzyme. Detailed kinetic studies of the fluorescence changes during the interaction of LM-4143 with apoCOX-2 were performed.

Kinetics of the Rapid Association of LM-4143 with ApoCOX-2 and ApoCOX-1. The rapid phase of fluorescence increase of LM-4143 with apoCOX-2 partially occurred within the dead time of the stopped-flow apparatus (∼1 ms), and the rapid fluorescence increase with apoCOX-1 occurred in less than 1 ms (Figure 5A). This precluded direct measurement of the rate of this phase of the process. However, as shown in Figure 6, addition of increasing amounts of LM-4143 to a fixed amount of apoCOX-2 led to an increase in the amplitude of the fluorescence change during the rapid phase. When the data were corrected for the background fluorescence of the inhibitor in the absence

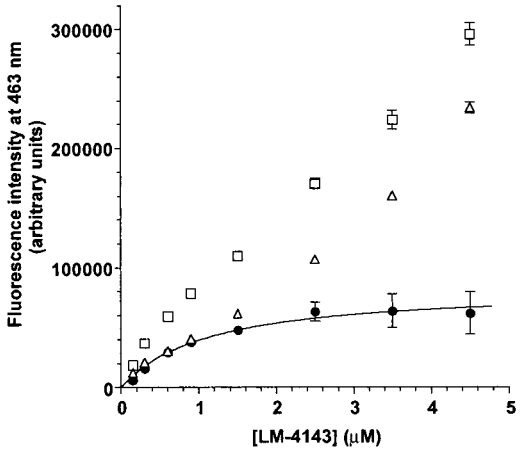

FIGURE 6: Analysis of the rapid fluorescence increase of LM-4143 with apoCOX-2. ApoCOX-2 (0.05 μM) was mixed with excess inhibitor, and the increase in the fluorescence intensity was recorded. The intensities of the inhibitor in buffer (triangles) were subtracted from those in the presence of apoenzyme (squares) to yield the intensities for the fluorescence change due to enzyme−inhibitor interaction (circles). The latter data were fitted to a hyperbolic equation to yield an apparent K_D. All data points represent the mean values ± SD of at least three independent measurements. Where error bars are not shown, they are smaller than the symbol size.

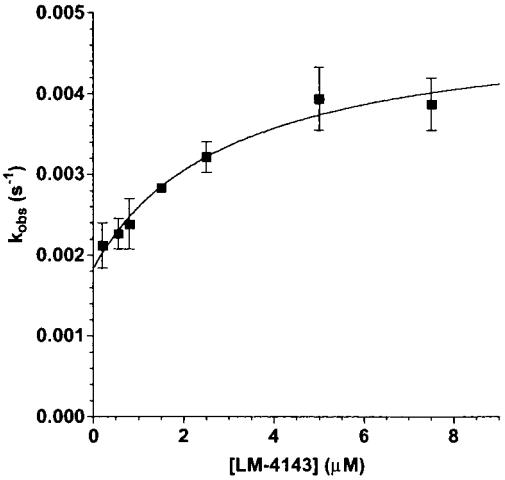

FIGURE 7: Kinetic analysis of the slow phase of the association of LM-4143 with apoCOX-2. The experiments were performed under conditions in which the change in free inhibitor concentration was less than 10%. The k_{obs} were obtained from single-exponential fits to kinetic traces of the slow fluorescence increase with apoCOX-2, as shown in Figure 5A. The k_{obs} were plotted versus inhibitor concentration and fitted to a hyperbolic equation with a floating *y*-intercept, as described in the text. The data points represent the mean values ± SD of three independent measurements, corrected for fluorescence of the inhibitor in buffer. Other details are provided under Materials and Methods.

of enzyme, a simple hyperbolic curve was obtained (Figure 6). These results suggest that the rapid fluorescence change of LM-4143 upon addition to apoCOX-2 represents a saturable interaction between the inhibitor and the protein. Nonlinear regression analysis of the data in Figure 6 produced a K_D value of 1.1 ± 0.4 μM for this apparent interaction. The K_D values obtained by titration of enzyme with a fixed concentration of LM-4143 or titration of LM-4143 with a fixed concentration of enzyme were not significantly different (data not shown). Substitution of apoCOX-1 for apoCOX-2 produced nearly identical results (K_D = 0.9 μM). Notably, the presence of the specific, nonfluorescent COX inhibitor, flurbiprofen, had no effect on the amplitude of the rapid fluorescence change of LM-4143 with either apoCOX-1 or apoCOX-2.

Kinetics of the Slow Fluorescence Increase in the Interaction of LM-4143 with ApoCOX-2. Following the rapid, initial fluorescence change observed upon addition of LM-4143 to apoCOX-2, a large additional increase in fluorescence was observed that developed more slowly. As stated above, a similar increase was not observed with apoCOX-1. The slow development of fluorescence was completely prevented by (*S*)-flurbiprofen (Figure 5A). When LM-4143 was added to apoCOX-2 under conditions in which the change in free inhibitor concentration was less than 10%, plots of the slow fluorescence change versus time fit a single-exponential function, yielding values for the observed first-order rate constant (k_{obs}) for the process. As shown in Figure 7, when values for k_{obs} obtained at different LM-4143 concentrations were plotted against LM-4143 concentration, a hyperbolic function with a nonzero *y*-intercept was obtained. These results, which were similar to those obtained from the time-dependent inhibition studies, suggested that the change in fluorescence observed during the interaction of LM-4143 with apoCOX-2 correlated with inhibition of enzyme activity. Further support for this interpretation comes from the finding that the values obtained for k_2, k_{-2}, and K_D by nonlinear regression analysis of the data in Figure 7, using eq 2, were similar to those obtained from the analysis of inhibition kinetics (Table 1).

The reversibility of the interaction of LM-4143 with apoCOX-2 was further explored in competition experiments with (*S*)-flurbiprofen (Figure 8). When (*S*)-flurbiprofen was added to the preformed LM-4143−apoCOX-2 complex, a decrease in fluorescence was observed that fit a single-exponential function. The amount of fluorescence remaining at the end of the process was equal to the fluorescence observed after the rapid interaction of LM-4143 with enzyme (Figure 8A). These data are consistent with the two equilibrium reactions, described above. Nonlinear regression analysis of the data in Figure 8A yielded a value of k_{-2} that agreed well with those obtained by evaluation of the slow phase increase in fluorescence (Figure 7, Table 1). With saturating (*S*)-flurbiprofen, the observed rate constants were independent of (*S*)-flurbiprofen concentration (Figure 8B), indicating that binding of (*S*)-flurbiprofen in the active site was not rate-limiting for competition with LM-4143.

Binding to and Inhibition of COX-2 Active Site Variants by LM-4143. Arg-120, Tyr-355, and Glu-524 comprise the constriction site in the COX-2 active site and are important residues for carboxylate binding. Previous studies have shown that these residues are also critical for the inhibitor potency of indomethacin esters and amides (*9*). Therefore, we tested the effects of several site-directed substitutions of these amino acids on the interaction of LM-4143 with COX-2. As indicated in Figure 9 and Table 3, mutation of any of the three residues (R120A, Y355A, Y355F, or E524L) eliminated the slow phase of inhibitor association as indicated by the change in fluorescence. Interestingly, an R120Q substitution did not produce this result (Figure 9, Table 3) and, in fact, appeared to enhance the rate and extent of the slow phase fluorescence change. In agreement with the binding kinetics, the potency of LM-4143 toward the constriction site variants decreased dramatically, as indicated

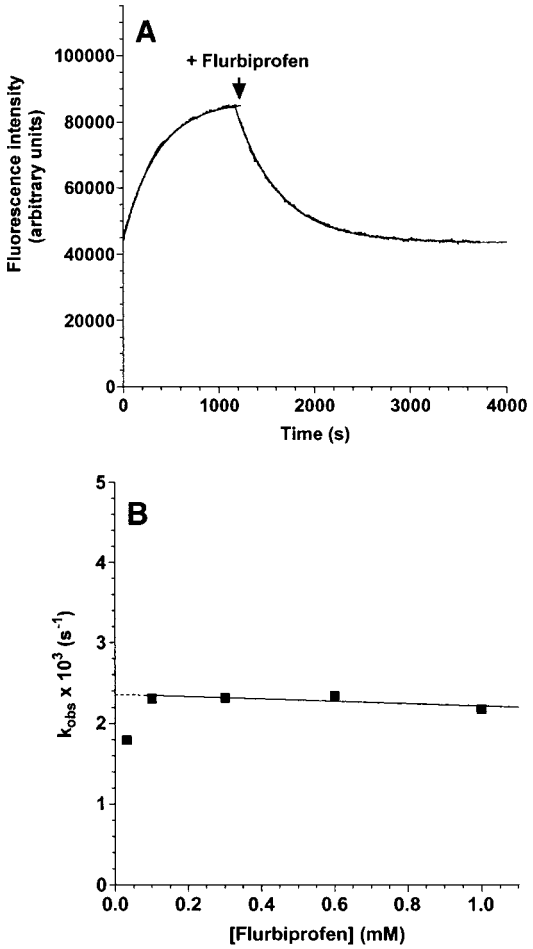

FIGURE 8: Competition of LM-4143, prebound to apoCOX-2, by (*S*)-flurbiprofen. (A) Kinetic traces of the fluorescence intensity of LM-4143 (0.2 μM) during incubation with apoCOX-2 (1 μM), followed by mixing with (*S*)-flurbiprofen (0.1 mM). The data sets for time-dependent fluorescence increase and decrease were background subtracted and fitted to a single-exponential equation, as described under Materials and Methods. (B) Effect of (*S*)-flurbiprofen concentration on the observed rate of fluorescence decrease in the above experiment.

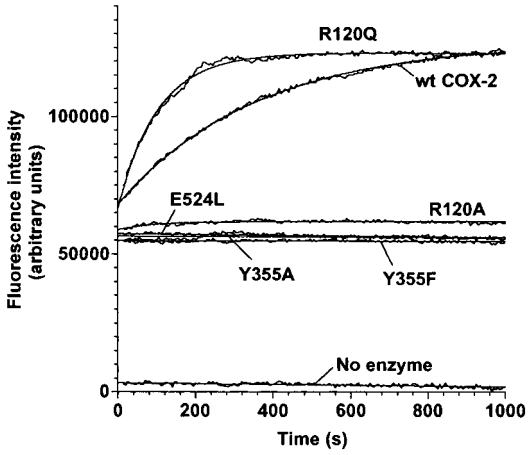

FIGURE 9: Effects of site-specific substitutions of amino acid residues in the substrate access channel of apoCOX-2 on the association kinetics with LM-4143. The fluorescence of the inhibitor (0.2 μM) was monitored upon mixing with apoenzyme (2 μM) or in buffer alone, as detailed under Materials and Methods. The data were background subtracted and fitted to a single-exponential equation or linear regression, as appropriate.

Table 3: Time-Dependent Binding and Inhibition of COX-2 Active Site Variants with LM-4143

enzyme	residual activity (%)[a]	binding by fluorescence[b]	
		amplitude	k_{obs} (s^{-1})
wt COX-2	47.0	1.00 ± 0.04	0.0028
R120Q	38.8	0.88± 0.16	0.0097
R120A	83.0	0.45± 0.04	0.011
Y355F	69.6	~0	–[c]
Y355A	85.4	~0	–[c]
E524L	85.2	~0	–[c]

[a] Residual activity was determined from cyclooxygenase activity remaining after a 20 min preincubation with 25 μM LM-4143 and is expressed as the percent of the activity without inhibitor. [b] Amplitudes and first-order rate constants for the fluorescence increase in the slow phase were determined from single-exponential fits to the data, as shown in Figure 9. Amplitudes were normalized by the amplitude with wild-type COX-2. Where not shown, the standard errors of the fits were less than 3% of the calculated amplitudes and less than 20% of the calculated rates. [c] No binding interaction was observed by fluorescence.

by residual enzyme activity in the presence of 25 μM LM-4143. Again, the R120Q mutant was the exception, showing inhibition to the same extent as wild-type COX-2 (Table 3). Neither the extent (Figure 9) nor the rate (not shown) of the rapid fluorescence increase was significantly affected by substituting constriction site residues.

DISCUSSION

In this study, fluorescent cinnamyl and coumarinyl groups were tethered to the hydroxyl group of *N*-indomethacinyl-ethanolamine to serve as probes of inhibitor−COX-2 interaction. We took advantage of a previous observation from our laboratory that a broad range of alkyl and aryl amides of indomethacin are highly selective COX-2 inhibitors. Indeed, both the cinnamyl (LM-4134) and coumarinyl (LM-4143) derivatives described herein are selective inhibitors of COX-2 although their potencies are not as great as some of the compounds previously described (*10*). These two fluorophores served as sensitive probes of polarity to monitor the inhibitor interaction with apoCOX-2 and its active site variants. The low fluorescence quantum yields of LM-4134 and LM-4143 in buffer may result from molecular aggregation, driven by hydrophobic interactions, and orientational relaxation of the excited state of the fluorophores by solvent (*24*). The former possibility is supported by anisotropy measurements made in this work and the previously reported solvent dependence of the fluorescence of fatty acid esters with variable chain length fatty acyl groups (*25*). Upon transfer of fluorescent indomethacin derivatives from buffer to relatively nonpolar binding sites on COX-1 or COX-2, the observed fluorescence increased dramatically. Although the fluorescence quantum yield of LM-4134, bound to COX-2, was similar to its quantum yield in acetonitrile, the quantum yield of enzyme-bound LM-4143 was higher than in acetonitrile. The greater fluorescence of protein-immobilized LM-4143 may be caused by a coplanar conformation of the diethylamino substituent relative to the coumarin ring, as reported previously (*26*). The fluorescence quantum yields, emission maxima, and anisotropy values indicated that, upon initial association, the indoamide molecules became immobilized on both COX-1 and COX-2 in a less polar environment, and the slow transition for the complex with apoCOX-2 further decreased the polarity of the environment around the indoamide molecules.

Upon addition of LM-4143 or LM-4134 to apoCOX-2, the absolute magnitude of the fluorescence increase was sufficiently great that this process could be monitored at concentrations of inhibitor and protein used in routine enzyme assays. This enabled a direct comparison of the kinetics of the fluorescence change with those of enzyme inactivation, which was most easily accomplished using the more highly fluorescent inhibitor, LM-4143. Addition of LM-4143 to apoCOX-2 led to a rapid increase in fluorescence, followed by a slower phase that obeyed first-order kinetics in the presence of excess inhibitor. Studies of the observed rate constants for the slow fluorescence increase indicated that the kinetics of this process were similar to the kinetics of the time-dependent inhibition of heme-reconstituted COX-2 by this compound. The data are consistent with the rapid formation of an initial complex followed by a slow, reversible unimolecular event that leads to enzyme inactivation and the slow phase fluorescence increase. The slow fluorescence change was not observed with apoCOX-1 nor did LM-4143 inhibit COX-1 activity. This indicates a close correlation between the slow step in enhancement of fluorescence of LM-4143 by apoCOX-2 and the slow step leading to enzyme inhibition.

The significance of the initial, rapid increase in fluorescence observed upon addition of LM-4143 to apoCOX-2 is unclear. Although this process occurred too quickly for direct kinetic study, evaluation of the magnitude of the rapid fluorescence change suggested that it represents a saturable binding interaction. Interestingly, the K_D value obtained for this apparent interaction was similar to the value for the initial interaction of enzyme with inhibitor obtained from analysis of either the slow phase fluorescence change or time-dependent enzyme inhibition. Thus, it is tempting to conclude that the rapid change in fluorescence corresponds to the formation of the initial enzyme−inhibitor complex as outlined in eq 1. It is notable, however, that this rapid fluorescence change occurs with apoCOX-1 as well as with apoCOX-2 and it does not correlate with enzyme inhibition. No competitive inhibition of COX-2 with LM-4143 was observed, and LM-4143 shows no inhibitor efficacy for COX-1. It is not blocked by (*S*)-flurbiprofen, it is not affected by the presence of heme in the enzyme, and it is not altered by mutations that eliminate the slow phase fluorescence change. Therefore, if the rapid fluorescence change does correspond to formation of the initial enzyme−inhibitor complex, we must conclude that the site of this interaction does not restrict access of the substrate to the active site, and it is not relevant to the isoform specificity of the inhibitor. It is notable that other time-dependent COX-2 inhibitors have been shown to interact with the enzyme in multistep equilibria in which the binding constant determined from time-dependent inhibition studies does not correlate with the binding constant determined from competitive inhibition studies (*9*, *21*).

The maximum k_{obs} value for the slow fluorescence enhancement or inhibition of COX-2 by LM-4143 was 1−2 orders of magnitude lower than those of the COX-2-selective inhibitors, SC299 (14), celecoxib, SC560, meloxicam, nimesulide (*21*), DuP-697, and NS-398 (12), as well as those reported for the nonselective NSAIDs, diclofenac and ketoprofen (*12*). The kinetically derived first-order inhibition rate constant was also 1−2 orders of magnitude lower with LM-4143 than with several diaryl heterocycles and NSAIDs (*12*, *21*, *27*) but was similar to those observed with piroxicam and meloxicam, both of which are reversible COX-2 inhibitors (*27*). It is interesting to note that the rate constant for inhibition of murine COX-2 by indomethacin is reported to be 0.045 s^{-1} (*27*), which is 7-fold higher than the rate determined for LM-4143. In addition, the rate of reversal of the slow binding and inhibition of COX-2 by LM-4143 is significantly faster than that of indomethacin, which is only very slowly reversible. Thus, inhibition by LM-4143, which is a moderately strong inhibitor of COX-2, is more readily reversible than that by indomethacin. This may reflect the importance of ion pairing in the tight binding of indomethacin, which is not possible in the amide derivative, and the presence of a moderately bulky coumarin ring tethered to the indomethacin indoamide.

The interaction of LM-4143 with residues at the constriction in the COX-2 active site appears to be critical for slow fluorescence enhancement and cyclooxygenase inhibition. These residues (Arg-120, Tyr-355, and Glu-524) form a hydrogen bond network that is proposed to control the binding dynamics of some NSAIDs and selective COX-2 inhibitors (*8*, *29*−*29*). Their substitution with nonpolar residues in the present study resulted in the loss of time-dependent binding and inhibition of COX-2 by LM-4143. However, the binding and inhibition of an R120Q mutant were similar to those of wild-type enzyme, further supporting the conclusion that hydrogen-bonding interactions are important for the binding of LM-4143 at the constriction site in COX-2. The structural nature of these interactions is undefined but may involve a complex network of hydrogen bonds between constriction site residues and the amide hydrogen of the LM-4143. Primary and secondary amides are potent inhibitors of COX-2 whereas tertiary amides are not (*9*).

The slow, unimolecular step in the binding of LM-4143 to COX-2 ($k = 0.003 \pm 0.001$ s^{-1}) is slower than the corresponding step in the binding of the diaryl heterocycle, SC299, to either COX-2 or COX-1 ($k \sim 0.1$ s^{-1}) (*14*). This step has been proposed to reflect the opening and closing of the constriction site to permit diaryl heterocycles to bind in the COX-2 active site. However, the rate constants must also reflect the structural reorganization required to permit enzyme−inhibitor association above the constriction. The steric demands of LM-4143 appear to slow this step substantially. As discussed above, an intermediate rate constant for inhibition of COX-2 has been reported for indomethacin ($k = 0.045$ s^{-1}) (*27*).

The pioneering work of Rome and Lands established that several potent NSAIDs are slow, tight-binding inhibitors of COX-1 (*22*). This discovery was extended by Copeland et al., who demonstrated that the selectivity of several diaryl heterocycles for COX-2 is manifest in a slow step that is not observed with COX-1 (*23*). The results of the present study of amide derivatives of indomethacin fit this paradigm and extend it to COX-2 selective inhibitors that are not diaryl heterocycles. The use of fluorescence techniques that allow real-time monitoring of inhibitor−enzyme association and dissociation has provided useful insights into the individual steps in binding (*12*−*14*). The results of such studies correspond closely to the results of detailed kinetic studies of inhibition (*21*). A general mechanism is emerging in which

multiple inhibitor−COX complexes (a minimum of two or three depending on inhibitor class) exist that are linked by sequential equilbria (e.g., eq 1) (*13*−*14*, *21*). The magnitude of the individual rate constants determines whether the inhibitor appears to be "time-dependent" and whether it is selective for one COX isoform in preference to the other.

ACKNOWLEDGMENT

The COX-2 active site mutants were generously provided by S. Rowlinson. We are grateful to K. Kozak for a critical reading of the manuscript.

REFERENCES

1. Marnett, L. J., and Kalgutkar, A. S. (1999) *Trends Pharmacol. Sci. 20*, 465−469.
2. Vane, J. R., Bakhle, Y. S., and Botting, R. M. (1998) *Annu. Rev. Pharmacol. Toxicol. 38*, 97−120.
3. Silverstein, F. E., Faich, G., Goldstein, J. L., Simon, L. S., Pincus, T., Whelton, A., Makuch, R., Eisen, G., Agrawal, N. M., Stenson, W. F., Burr, A. M., Zhao, W. W., Kent, J. D., Lefkowith, J. B., Verburg, K. M., and Geis, G. S. (2000) *J. Am. Med. Assoc. 284*, 1247−1255.
4. Laine, L., Harper, S., Simon, T., Bath, R., Johanson, J., Schwartz, H., Stern, S., Quan, H., and Bolognese, J. (1999) *Gastroenterology 117*, 776−783.
5. Penning, T. D., Talley, J. J., Bertenshaw, S. R., Carter, J. S., Collins, P. W., Docter, S., Graneto, M. J., Lee, L. F., Malecha, J. W., Miyashiro, J. M., Rogers, R. S., Rogier, D. J., Yu, S. S., Anderson, G. D., Burton, E. G., Cogburn, J. N., Gregory, S. A., Kobolt, C. M., Perkins, W. E., Siebert, K., Veenhuizen, A. W., Zhang, Y. Y., and Isakson, P. C. (1997) *J. Med. Chem. 40*, 1347−1365.
6. Prasit, P., Wang, Z., Brideau, C., Chan, C. C., Charleson, S., Cromlish, W., Ethier, D., Evans, J. F., Ford-Hutchinson, A. W., Gauthier, J. Y., Gordon, R., Guay, J., Gresser, M., Kargman, S., Kennedy, B., Leblanc, Y., Léger, S., Mancini, J., O'Neill, G. P., Ouellet, M., Percival, M. D., Perrier, H., Riendeau, D., and Rodger, I. (1999) *Bioorg. Med. Chem. Lett. 9*, 1773−1778.
7. Kurumbail, R. G., Stevens, A. M., Gierse, J. K., McDonald, J. J., Stegeman, R. A., Pak, J. Y., Gildehaus, D., Miyashiro, J. M., Penning, T. D., Seibert, K., Isakson, P. C., and Stallings, W. C. (1996) *Nature 384*, 644−648.
8. Luong, C., Miller, A., Barnett, J., Chow, J., Ramesha, C., and Browner, M. F. (1996) *Nat. Struct. Biol. 3*, 927−933.
9. Kalgutkar, A. S., Crews, B. C., Rowlinson, S. W., Marnett, A. B., Kozak, K. R., Remmel, R. P., and Marnett, L. J. (2000) *Proc. Natl. Acad. Sci. U.S.A. 97*, 925−930.
10. Kalgutkar, A. S., Marnett, A. B., Crews, B. C., Remmel, R. P., and Marnett, L. J. (2000) *J. Med. Chem. 43*, 2860−2870.
11. Kalgutkar, A. S., Rowlinson, S. W., Crews, B. C., and Marnett, L. J. (2002) *Bioorg. Med. Chem. Lett. 25*, 521−524.
12. Houtzager, V., Ouellet, M., Falgueyret, J. P., Passmore, L. A., Bayly, C., and Percival, M. D. (1996) *Biochemistry 35*, 10974−10984.
13. Lanzo, C. A., Beechem, J., Talley, J., and Marnett, L. J. (1998) *Biochemistry 37*, 217−226.
14. Lanzo, C. A., Sutin, J., Rowlinson, S. W., Talley, J., and Marnett, L. J. (2000) *Biochemistry 39*, 6228−6234.
15. Marnett, L. J., Siedlik, P. H., Ochs, R. C., Pagels, W. D., Das, M., Honn, K. V., Warnock, R. H., Tainer, B. E., and Eling, T. E. (1984) *Mol. Pharmacol. 26*, 328−335.
16. Rowlinson, S. W., Crews, B. C., Lanzo, C. A., and Marnett, L. J. (1999) *J. Biol. Chem. 274*, 23305−23310.
17. Velapoldi, R. A. (1972) *J. Res. Natl. Bur. Stand. 76A*, 641−654.
18. Tairi, A. P., Hovius, R., Pick, H., Blasey, H., Bernard, A., Surprenant, A., Lundstrom, K., and Vogel, H. (1998) *Biochemistry 37*, 15850−15864.
19. Badea, M. G., and Brand, L. (1979) *Methods Enzymol. 61*, 378−425.
20. Strickland, S., Palmer, G., and Massey, V. (1975) *J. Biol. Chem. 250*, 4048−4052.
21. Walker, M. C., Kurumbail, R. G., Kiefer, J. R., Moreland, K. T., Koboldt, C. M., Isakson, P. C., Seibert, K., and Gierse, J. K. (2001) *Biochem. J. 357*, 709−718.
22. Rome, L. H., and Lands, W. E. M. (1975) *Proc. Natl. Acad. Sci. U.S.A. 72*, 4863−4865.
23. Copeland, R. A., Williams, J. M., Giannaras, J., Nurnberg, S., Covington, M., Pinto, D., Pick, S., and Trzaskos, J. M. (1994) *Proc. Natl. Acad. Sci. U.S.A. 91*, 11202−11206.
24. Slavik, J. (1994) *Fluorescent Probes in Cellular and Molecular Biology*, pp 128−129, CRC Press, Boca Raton, FL.
25. Lloyd, J. B. F. (1979) *J. Chromatogr. 178*, 249−258.
26. Hirshberg, M., Henrick, K., Haire, L. L., Vasisht, N., Brune, M., Corrie, J. E., and Webb, M. R. (1998) *Biochemistry 37*, 10381−10385.
27. Gierse, J. K., Koboldt, C. M., Walker, M. C., Seibert, K., and Isakson, P. C. (1999) *Biochem. J. 339*, 607−614.
28. So, O.-Y., Scarafia, L. E., Mak, A. Y., Callan, O. H., and Swinney, D. C. (1998) *J. Biol. Chem. 273*, 5801−5807.
29. Bhattacharyya, D. K., Lecomte, M., Rieke, C. J., Garavito, R. M., and Smith, W. L. (1996) *J. Biol. Chem. 271*, 2179−2184.

BI0203637